



Cite this: *Dalton Trans.*, 2015, **44**, 16332

## Unexpected DNA binding properties with correlated downstream biological applications in mono vs. bis-1,8-naphthalimide Ru(II)-polypyridyl conjugates†

Gary J. Ryan,<sup>a</sup> Fergus E. Poynton,<sup>a</sup> Robert B. P. Elmes,<sup>‡a</sup> Marialuisa Erby,<sup>b</sup> D. Clive Williams,<sup>\*b</sup> Susan J. Quinn<sup>\*c</sup> and Thorfinnur Gunnlaugsson<sup>\*a</sup>

The synthesis, spectroscopic characterisation and biological evaluation of mono- and bis-1,8-naphthalimide-conjugated ruthenium(II)-polypyridyl complexes is presented. Spectroscopic DNA titrations, together with denaturation studies, show strong binding of both species to DNA through the naphthalimide arms. Linear and circular dichroism (LD and CD) spectroscopy reveal close association of the Ru(bpy)<sub>3</sub><sup>2+</sup> core with DNA in the case of the mono-naphthalimide complex, [Ru(bpy)<sub>2</sub>(bpy-NAP)]<sup>2+</sup>. Significantly, binding by the second naphthalimide arm in the [Ru(bpy)<sub>2</sub>(bpy-NAP<sub>2</sub>)]<sup>2+</sup> complex is found to displace the Ru(bpy)<sub>3</sub><sup>2+</sup> centre from the DNA backbone. This 'negative allosteric effect' is found to have a dramatic influence on the photoinduced damage of plasmid DNA, and the viability of HeLa cancer cells upon photoactivation. Overall the study clearly maps and correlates the relationship between molecular structure, *in vitro* binding and activity, and *in cellulo* function.

Received 26th January 2015,  
Accepted 5th August 2015

DOI: 10.1039/c5dt00360a

www.rsc.org/dalton

### Introduction

The development of transition metal polypyridyl complexes capable of targeting DNA has been extensively investigated in recent times.<sup>1–5</sup> This has been largely motivated by the desire to probe DNA-based chemical processes with the view of developing novel therapeutic agents.<sup>6–8</sup> Ru(II)-polypyridyl complexes show particular promise due to their water solubility, chemical and kinetic inertness and spectroscopic properties such as visible light absorbance and photoluminescence.<sup>4,9</sup> They have been shown to be internalised by cells, with a variety of mechanisms proposed including endocytosis, active transport and passive diffusion, or through the use of vectors or delivery molecules such as polypeptides.<sup>10–13</sup> Tuning the polypyridyl ligand structure confers diverse functionality leading to intercalating complexes capable of 'light-switching' signalling phenomena, and strong DNA binding and photoinduced reactivity with

DNA.<sup>14–19</sup> Furthermore, we have recently shown that such complexes, based on simple bpy and phen ligands, when conjugated *via* an alkyl thio-linker to the surface of gold nanoparticles can be employed for luminescent imaging within cancer cells.<sup>20</sup> We are interested in combining these features to develop molecules as dual imaging and therapeutic agents. Molecules can bind to DNA through a number of modes.<sup>6,7,21</sup> Ru(II)-polypyridyl systems have been shown to bind to DNA by various modes, *e.g.* through intercalation, groove binding and electrostatic interactions.<sup>22–29</sup> We have also developed several examples of DNA targeting binders, based on the use of 1,8-naphthalimide derivatives.<sup>30–38</sup> Such structures have tuneable electronic properties, and have been shown to exhibit good DNA binding affinity through either intercalation or groove binding.<sup>39–44</sup> In addition to being effective DNA intercalators or groove binders, the 1,8-naphthalimides can also act as sensitising antenna for the Ru(II)-based metal-to-ligand charge transfer (MLCT) emission, allowing for the population of the excited state using two excitation channels.<sup>45</sup> Herein, we present two new DNA targeting Ru(II) complexes, [Ru(bpy)<sub>2</sub>(bpy-NAP)]<sup>2+</sup> (**Ru-Nap**) and [Ru(bpy)<sub>2</sub>(bpy-NAP<sub>2</sub>)]<sup>2+</sup> (**Ru-2Nap**), Fig. 1, based on the conjugation of one or two 1,8-naphthalimide units, respectively, to the polypyridyl complexes *via* a flexible alkyl spacer. The rational design of these complexes is based on combining (a) the DNA affinity and (b) the lipophilic nature of the naphthalimide group to facilitate more efficient binding of such Ru(II) complexes to

<sup>a</sup>School of Chemistry and Trinity Biomedical Sciences Institute (TBSI), Trinity College Dublin, Dublin 2, Ireland. E-mail: gunnlaut@tcd.ie

<sup>b</sup>School of Biochemistry and Immunology, and Trinity Biomedical Sciences Institute (TBSI), Trinity College Dublin, Dublin 2, Ireland. E-mail: clive.williams@tcd.ie

<sup>c</sup>School of Chemistry and Chemical Biology, University College Dublin, Dublin 4, Ireland. E-mail: susan.quinn@ucd.ie

†Electronic supplementary information (ESI) available. See DOI: 10.1039/c5dt00360a

‡Current address: Department of Chemistry, Maynooth University, National University of Ireland, Maynooth, Co. Kildare, Ireland.

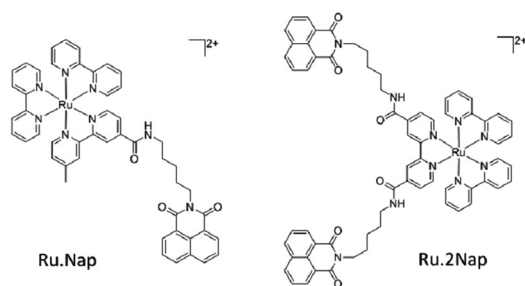


Fig. 1 The Ru(II) based naphthalimide complexes **Ru-Nap** and **Ru-2Nap**.

DNA in a cooperative manner,<sup>38</sup> and potentially enhance cellular uptake.<sup>36</sup> To fully explore the activity of the complexes a detailed *in vitro* photophysical study was completed in the absence and presence of DNA.

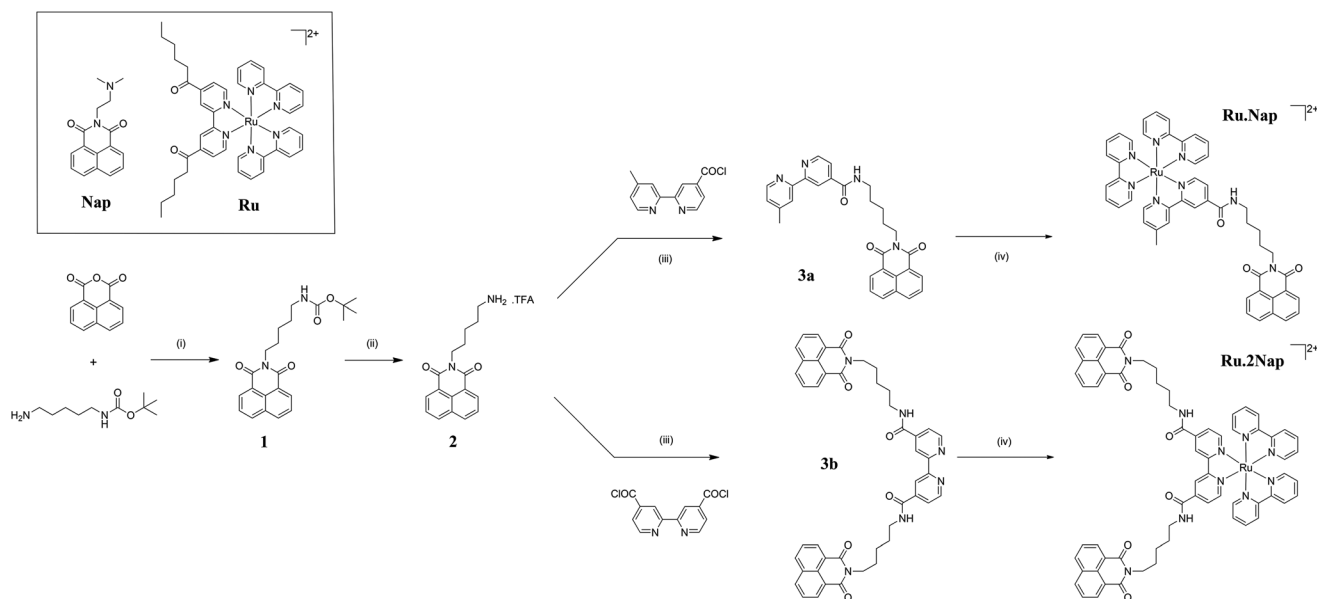
Two distinct ligand-dependant DNA binding modes were observed. In the mono-naphthalimide complex intercalation of the naphthalimide brings the Ru(II)-polypyridyl centre in close proximity to the DNA sugar phosphate backbone, which facilitates efficient DNA cleavage upon photoirradiation. However, then in the case of **Ru-2Nap** the binding interaction of the second naphthalimide arm to DNA, reduces interaction of the Ru(II)-polypyridyl centre with the DNA backbone. Consequently, this complex is found to be a less effective photocleavage agent. This 'negative allosteric effect' leads to different biological activity of the **Ru-Nap** and **Ru-2Nap** complexes within HeLa cervical cancer cells and demonstrates how a simple design modification to the polypyridyl ligand can lead to modulated photophysical properties and downstream

biological activity of such Ru(II)-polypyridyl-naphthalimide conjugates. This phenomenon, has to the best of our knowledge, not been demonstrated before for such systems and can have significant consequences on the 'function' or application (*i.e.* therapeutic *vs.* diagnostic) of such complexes in chemical biology.

## Results and discussion

### Synthesis of **Ru-Nap** and **Ru-2Nap**

The mono-substituted naphthalimide complex **Ru-Nap** and the bis-substituted complex **Ru-2Nap** were synthesised in high yield, as demonstrated in Scheme 1. Firstly, the 1,8-naphthalimide **1**, was formed using the mono-protected Boc diamine, *N*-(*tert*-butoxycarbonyl)-1,5-diaminopentane, giving **2** after BOC-deprotection using TFA. The naphthalimide **2** was then reacted with the appropriate 2,2'-bipyridine acid chloride under anhydrous conditions to give **3a** and **3b** in 83 and 95% yield, respectively, after initial aqueous acid workup, followed by further purification using silica column chromatography. This was followed by complexation of **3a** and **3b** with Ru-(bpy)<sub>2</sub>Cl<sub>2</sub>. For both, the reaction mixture was heated at reflux under an argon atmosphere for 20 h, followed by purification involving, treatment with concentrated aqueous solution of NH<sub>4</sub>PF<sub>6</sub>, which resulted in the formation of the PF<sub>6</sub><sup>-</sup> salts. These were purified using silica flash column chromatography by eluting the sample using the solvent mixture CH<sub>3</sub>CN : H<sub>2</sub>O : NaNO<sub>3</sub>(sat) (40 : 4 : 1). The Cl<sup>-</sup> salts of these complexes were then regenerated by stirring a solution of either **Ru-Nap** and **Ru-2Nap** in MeOH with Amberlite ion exchange resin. The Cl<sup>-</sup> salts were then further purified by column chromatography on



Scheme 1 Synthesis of **Ru-Nap** and **Ru-2Nap**. Reagents and conditions: (i) anhyd. toluene, Et<sub>3</sub>N, reflux 24 h (ii) TFA/CH<sub>2</sub>Cl<sub>2</sub> 1 : 1, RT 1 h, (iii) dry CH<sub>2</sub>Cl<sub>2</sub>, Et<sub>3</sub>N, RT 12 h, (iv) Ru(bpy)<sub>2</sub>Cl<sub>2</sub>, DMF/H<sub>2</sub>O, Ar, reflux, 24 h to yield **Ru-NAP** (86%) and **Ru-2Naph** (76%). Inset: controls, **Ru** and **Nap**, synthesised for this study.

Sephadex LH-20, eluting with MeOH, giving the products as red/brown solids in 86 and 76% yields, respectively. Both **Ru-Nap** and **Ru-2Nap** were fully characterised (See Experimental). The distinct units of the complexes were readily discerned by NMR ( $\text{CD}_3\text{CN}$  and  $\text{CD}_3\text{OD}$ , 400 MHz) (See ESI Fig. S1–S7†). CHN analysis showed the formation of the desired products in high purity.

### UV-vis absorption spectra

Having successfully synthesised both **Ru-Nap** and **Ru-2Nap** their various photophysical properties were evaluated. The UV-vis absorption spectra were recorded in buffered pH 7.0 aqueous solution, and show distinctive spectroscopic signals for both the Ru(II) MLCT-based absorption and that of the naphthalimide, see Fig. 2a and b. In the case of **Ru-Nap** an intense band was observed at 286 nm, which was mainly attributed to  $\pi\text{-}\pi^*$  intraligand (IL) transitions. The band at 338 nm was assigned to the  $\pi\text{-}\pi^*$  1,8-naphthalimide transitions and the visible absorption band at 459 nm to the MLCT transitions of the Ru(II) centre. The presence of the amide substituted bipyridine ligands causes the MLCT band to be somewhat broadened and red shifted compared to that of  $\text{Ru}(\text{bpy})_3^{2+}$ .<sup>46</sup> In the case of the bis-naphthalimide system **Ru-2Nap** the presence of the additional amide group results in a shift in the bands at 338 and 459 nm to 345 and 480 nm respectively, see Fig. 2b. 1,8-Naphthalimides are known to interact through  $\pi$ -stacking and in **Ru-2Nap** this can occur intramolecularly between the two naphthalimides, or between

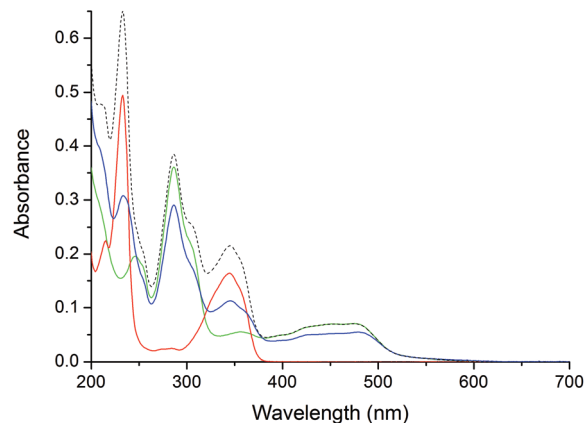


Fig. 3 UV/visible absorption spectra of **Ru-2Nap** (6.5  $\mu\text{M}$ ) (—), **Ru** (6.5  $\mu\text{M}$ ) (—), **Nap** (13  $\mu\text{M}$ ) (—) and **Ru + Nap** (-----). All samples recorded in 10 mM phosphate buffer at pH 7.

a naphthalimide and a bipyridine ligand.<sup>47,48</sup> For this reason, the existence of electronic interactions in the ground state were considered by constructing an additive spectrum using a suitable Ru(II) complex, **Ru** and a water soluble 1,8-naphthalimide derivative, **Nap**, see Fig. 3. Comparison of the summed spectra with that of **Ru-2Nap** reveals a number of differences. Firstly, the MLCT region is found to be less absorbing (by 22%) in **Ru-2Nap**. This strongly suggests electronic interaction between the Ru(II) centre and the 1,8-naphthalimide in the ground state. It is also worth noting that the IL transitions at 286 nm are also affected. Secondly, the band hypochromism was found to be more pronounced in the region of the 1,8-naphthalimide absorptions, at 230 and 345 nm, respectively. In particular, the absorbance at 345 nm is reduced by *ca.* 47%, in comparison to that observed for the additive spectrum. These observations suggest that significant intramolecular stacking interactions of the 1,8-naphthalimides occur in solution.<sup>49</sup>

### Emission spectra

Excitation of **Ru-Nap** and **Ru-2Nap** at 450 nm results in single band emission at 645 and 670 nm respectively, see Fig. 2. The amide substituted bipyridine ligands results in a red-shifted emission compared to that observed for  $\text{Ru}(\text{bpy})_3^{2+}$ , which typically emits at *ca.* 605 nm.<sup>50</sup> For both complexes significant contribution to MLCT-based emission is observed upon naphthalimide excitation, which suggests the presence of efficient singlet-singlet energy transfer, from the <sup>1</sup>naphthalimide to the <sup>1</sup>MLCT excited state. Evidence for this is clearly seen in the excitation spectra of these derivatives, see Fig. 2a and b, and by comparing these excitation spectra to that of the control **Ru** complex (See ESI Fig. S8†). Indeed, the absorption and excitation spectra are close to being super-imposable. The contribution to the Ru(II) emission from the 1,8-naphthalimides was found to be much greater for **Ru-2Nap** than **Ru-Nap**, which indicates that the second 1,8-naphthalimide

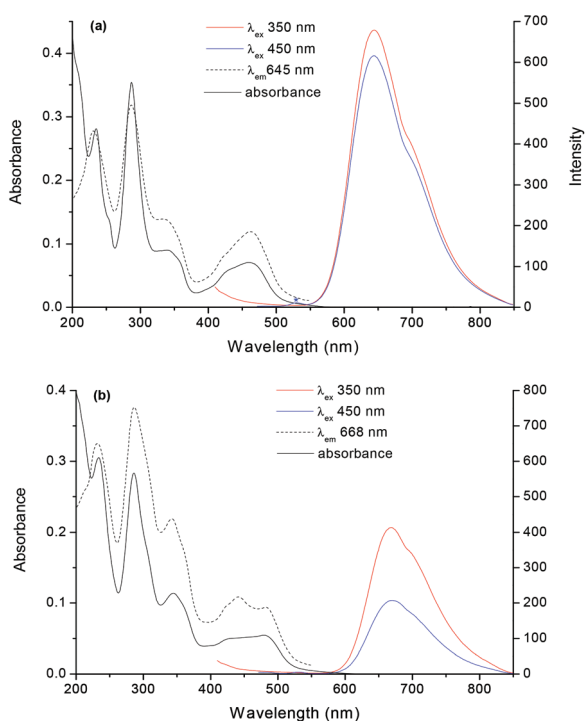


Fig. 2 UV/visible, excitation and emission spectra of (a) **Ru-Nap** (6.5  $\mu\text{M}$ ) and (b) **Ru-2Nap** (6.5  $\mu\text{M}$ ) in 10 mM phosphate buffer, at pH 7.

**Table 1** Emission properties of Ru(II) complexes in aerated and degassed solution at 298 K. All at 6.5  $\mu\text{M}$  concentration.  $\lambda_{\text{ex}}$  450 nm

Complex	$\lambda_{\text{em}}$ (nm)	$\Phi_{\text{f}}$ ( $\pm 10\%$ ) aerated buffer	$\Phi_{\text{f}}$ ( $\pm 10\%$ ) aerated acetonitrile	$\Phi_{\text{f}}$ ( $\pm 10\%$ ) de-gassed acetonitrile
<b>Ru</b>	670	0.014	0.021	0.061
<b>Ru-Nap</b>	645	0.018	—	—
<b>Ru-2Nap</b>	670	0.014	0.021	0.064

enhances this effect. The observation of very weak naphthalimide emission for both complexes is a further indication of energy transfer to the Ru(II)-polypyridyl centre. This process is represented schematically in Fig. S9 ESI.†

The quantum yields for both systems, recorded in buffered aqueous solution, compared well with that obtained for the control **Ru**  $\Phi_{\text{Ru-MLCT}} = 0.014$  (all excitation at 450 nm), see Table 1. These results confirm the absence of any quenching of the MLCT based emission by the naphthalimide, which is expected as the naphthalimide centre is not sufficiently oxidising to accept an electron from the excited states of the Ru(II) complex (as deduced from a simplified Rehm–Weller equation, where the driving force for electron transfer was calculated to be approximately 0.12 eV for **Ru-Nap** and 0.26 eV for **Ru-2Nap**, see ESI eqn (S1)†).<sup>51</sup> The positive free energy changes calculated for both systems render electron transfer from the excited Ru(II) complex to the 1,8-naphthalimide thermodynamically unfavourable in both cases. Quantum yield determination for **Ru-2Nap** in dry acetonitrile under aerated and degassed conditions revealed the complex emission to be quenched by dissolved oxygen (Table 1). Furthermore, the close agreement in the quantum yield values determined for **Ru-2Nap** and **Ru** suggests the absence of an equilibrium between the triplet excited state of the 1,8-naphthalimide and that of the Ru(II) complex. The presence of such equilibrium would be expected to greatly enhance the lifetime of **Ru-2Nap** over that of the reference complex. Having established the steady-state spectroscopic properties, the complexes were next studied in the presence of DNA to establish the influence of binding interactions.

### DNA binding: absorption titrations

The DNA binding properties of the complexes was probed by monitoring absorption bands of the naphthalimide and the Ru(II) centre. In the case of the mono-naphthalimide **Ru-Nap**, the addition of increasing concentrations of salmon testes' DNA (st-DNA) resulted in a 37% hypochromism of the 1,8-naphthalimide band at 338 nm (Fig. 4a). Such a large change in the absorbance is characteristic of intercalation.<sup>35,36,40,41</sup> A significant change was also observed in the absorbance of the MLCT band, which decreased by 16%. In comparison the control **Ru** complex undergoes a 9% hypochromic shift at the MLCT band, which is attributed to electrostatic interactions with the phosphate backbone of DNA.<sup>27</sup> The intrinsic binding constant of  $9.0 \times 10^6 \text{ M}^{-1}$  was derived from a binding isotherm

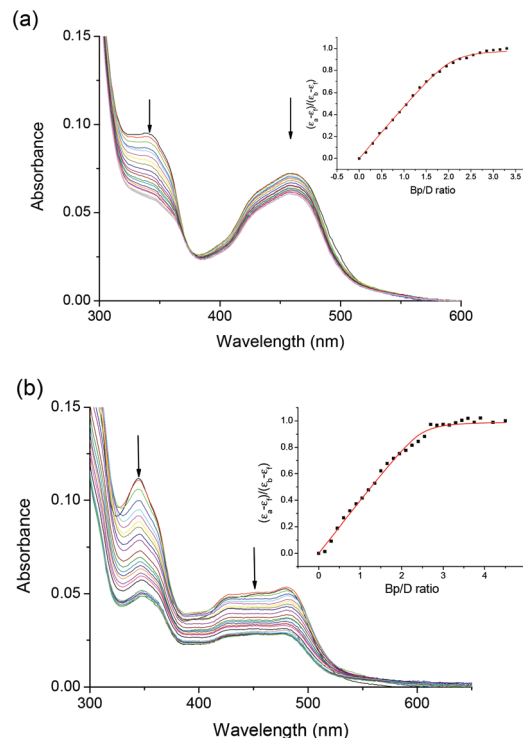


**Fig. 4** Changes in the UV/vis spectrum of (a) **Ru-Nap** (6.5  $\mu\text{M}$ ) upon addition of st-DNA (0–21.45  $\mu\text{M}$  base pairs) and (b) **Ru-2Nap** (6.7  $\mu\text{M}$ ) upon addition of st-DNA (0–29.25  $\mu\text{M}$  base pairs), in 10 mM phosphate buffer, pH 7. Inset: Plot of  $(\epsilon_{\text{a}} - \epsilon_{\text{i}})/(\epsilon_{\text{b}} - \epsilon_{\text{i}})$  at (a) 350 nm and (b) 355 nm vs. equivalents of DNA and the corresponding non-linear fit.

**Table 2** DNA binding parameters from fits to absorbance data

Complex	$\lambda(\text{Nap})$ $\Delta\text{Abs}$	$\lambda(\text{MLCT})$ $\Delta\text{Abs}$	Binding constant $K (\text{M}^{-1})$	Binding site size (base pairs)
<b>Ru-Nap</b>	37%	16%	$9.0 \times 10^6 (\pm 1.0) \text{ M}^{-1}$	2.18( $\pm 0.02$ )
<b>Ru-2Nap</b>	56%	41%	$1.5 \times 10^7 (\pm 0.5) \text{ M}^{-1}$	2.48( $\pm 0.02$ )

using the model of Bard *et al.*<sup>52</sup> and a binding site size of 2.18 base pairs was calculated, see Table 2. This is an order of magnitude higher than the binding observed for either the naphthalimide **Nap** or ruthenium metal centre,  $\text{Ru}(\text{bpy})_3^{2+}$ , **Ru** separately and confirms the presence of cooperative binding.

When the titration was repeated for **Ru-2Nap** even greater changes in the absorption spectrum were observed, see Fig. 4b. A large, 56%, hypochromic shift was observed in the naphthalimide band at 345 nm. However, more strikingly, a 41% decrease was observed for the MLCT band. The magnitude of the hypochromic shift is more than twice that observed for the mono-naphthalimide complex. These observations show that the environment of both the naphthalimide and the metal centre of **Ru-2Nap** is significantly altered in the presence of DNA, which also is the case for **Ru-Nap**. While, partial intercalation of the Ru(II) complex may also be possible, it is

unlikely due to the minimal extended planar nature of the bipyridine ligands.<sup>27</sup> The binding constant  $K$  for these interactions was determined as  $1.5 \times 10^7 \text{ M}^{-1}$ , with a slightly larger calculated binding site size of 2.48 base pairs. The binding curve profiles obtained from the UV-visible titrations indicate that both complexes bind very strongly to DNA. Notably, in the case of **Ru-2Nap** changes in the UV-vis absorption spectra are complicated by the existence of intramolecular  $\pi$ -stacking interactions between the naphthalimides and/or with the bpy ligand to which they are coupled. Furthermore, the lack of a clear isosbestic point in the case of **Ru-2Nap** possibly reflects the fact that the flexible linker allows multiple modes of binding to occur.

### DNA binding: emission titrations

Fluorometric DNA titrations were followed by exciting both chromophores independently at 338 nm and 450 nm. Having observed that the emission from the Ru(II) centre is sensitised by energy transfer from the 1,8-naphthalimides, it was expected that any intercalation of the naphthalimide group with DNA would result in changes in the photophysical properties of the complexes. Direct excitation of **Ru-Nap** metal centre at 450 nm resulted in a two phase increase in intensity coinciding with a more gradual increase after the addition of *ca.* one base pair equivalent. The emission was found to plateau at *ca.* 10 base pair equivalents with an increase in MLCT emission intensity of 20% observed (Fig. S10 ESI†). It is possible that the modest increase in intensity observed for **Ru-Nap**, is due to protection of the metal centre from quenching by oxygen and solvent molecules upon DNA binding.

MLCT emission observed upon excitation of the **Ru-Nap** naphthalimide group at 338 nm, in the presence of DNA, was found to decrease (*ca.* -43%) in intensity (Fig. S11 ESI†). A large decrease in intensity was observed up to the addition of *ca.* 3 base pair equivalents, followed by a more gradual decrease up to *ca.* 15 base pairs. No concomitant changes were seen in the 1,8-naphthalimide emission. We can consider that the binding of the naphthalimide, in the **Ru-Nap** complex, to DNA results in (1) positioning of the naphthalimide in a new chemical environment and (2) the disruption of coupling between the metal complex centre and naphthalimide. The effect on the intramolecular coupling is most clearly seen by comparing the excitation spectra of the complexes recorded in the presence, and absence of DNA (see Fig. 5). It can be seen that in the presence of higher concentrations of DNA the excitation spectrum for **Ru-Nap** closely resembles that of **Ru**, which has no appended 1,8-naphthalimides.

**Ru-2Nap** in the presence of DNA also exhibited complex emission behaviour. Direct excitation of the MLCT band at 450 nm in the presence of low concentrations of st-DNA (0–0.45 base pair equivalents) resulted in a modest (25%) increase in the MLCT emission intensity (Fig. S12 ESI†). However, in contrast to **Ru-Nap**, further additions of st-DNA resulted in a decrease in the emission intensity. The final intensity represented a decrease of 46% from that of the initial intensity. In **Ru-2Nap** excitation of the 1,8-naphthalimide band

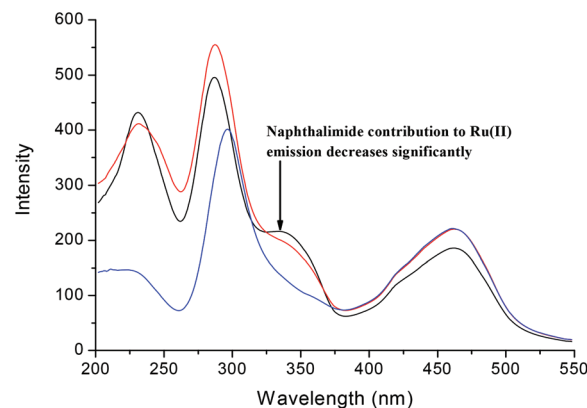


Fig. 5 Excitation spectrum of **Ru-Nap** ( $6.5 \mu\text{M}$ ) ( $\lambda_{\text{em}} = 645 \text{ nm}$ ) in 10 mM phosphate buffer, at pH 7 in the absence (—) and presence of st-DNA at a Bp/D ratio of 1 (—) and 20 (—).

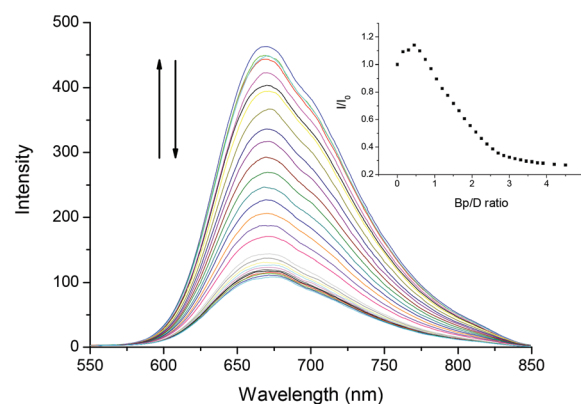


Fig. 6 (a) Changes in the emission spectrum ( $\lambda_{\text{ex}} = 345 \text{ nm}$ ) of **Ru-2Nap** ( $6.7 \mu\text{M}$ ) in 10 mM phosphate buffer, pH 7 with increasing concentration of st-DNA (0–60.3  $\mu\text{M}$ ).

at 345 nm yields more pronounced changes in emission intensity, see Fig. 6. An initial increase in intensity (14%) was observed at base equivalents (up to 0.45 base pairs), followed by a subsequent decrease of 73% compared to the initial intensity. The behaviour at low Bp/D equivalents is attributed to the disruption of intramolecular stacking of the 1,8-naphthalimides, which occurs in the presence of a small quantity of DNA. This unstacking is proposed to result in more efficient energy transfer to the metal.

The overall decrease in intensity may be attributed to quenching of the 1,8-naphthalimide singlet excited state by electron transfer from the nucleotides.<sup>40</sup> However, in the absence of electron transfer from a suitable nucleotide the decrease in intensity may also arise due to disruption of energy transfer from the naphthalimide to the metal centre due to the presence of the DNA environment as observed in the excitation spectrum (Fig. S13 ESI†).

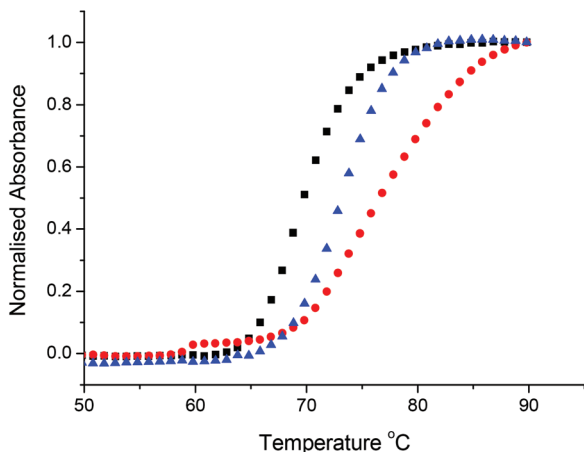


Fig. 7 Thermal denaturation curves of st-DNA (150  $\mu\text{M}$ ) in 10 mM phosphate buffer, at pH 7, in the absence (■) and the presence of **Ru·Nap** (●) and **Ru-2Nap** (▲) at a Bp/D ratio of 5.

### Thermal denaturation studies

Thermal denaturation studies were carried out to further elucidate the nature of the interaction of **Ru·Nap** and **Ru-2Nap** with DNA. Significant differences in the shifts in the melting temperature ( $T_m$ ) of DNA were observed in the presence of either complex. The presence of **Ru·Nap** resulted in an increase in  $T_m$  from 69  $^{\circ}\text{C}$  to 75.8  $^{\circ}\text{C}$  giving a  $\Delta T_m$  of 6.8  $^{\circ}\text{C}$ , see Fig. 7.

However, a much smaller stabilisation was observed with **Ru-2Nap**, giving a shift in  $T_m$  of 2  $^{\circ}\text{C}$ . These results suggest that **Ru·Nap** binds by a classical intercalative mode but indicate that **Ru-2Nap** binds in a non-classical mode, such as partial intercalation and groove binding of the two 1,8-naphthalimides, which may not stabilise the helix to the same extent. Given that the stabilisation of the DNA is expected to be enhanced by electrostatic interactions of the  $\text{Ru}(\text{bpy})_3^{2+}$  core with the DNA backbone, the reduced stabilisation observed for **Ru-2Nap** compared to **Ru·Nap** could be due to a change in the interaction of the metal complex with DNA.

### Circular dichroism (CD) and linear dichroism (LD) studies

Circular and linear dichroism<sup>53</sup> DNA titrations were also carried out for both complexes to determine the nature of any induced chirality in the presence of DNA and to attempt to elucidate their specific mode of DNA interaction. Keeping the concentration of DNA constant, increased amounts of the complexes were added to give a range of Bp/D ratios. Both conjugates were found to display similar CD behaviour. In the case of **Ru·Nap** a small induced CD signal was observed at long wavelength with the maximum appearing at approximately 470 nm for the MLCT absorption band, see Fig. 8a. This observation confirms that the  $\text{Ru}(\text{II})$  component of **Ru·Nap** is associated with the DNA structure. A small induced CD signal was observed in the region of absorption of the 1,8-naphthalimide at 350 nm, however larger signal changes were observed at lower wavelengths where absorption arises due to both the

naphthalimide and bpy  $\pi$ - $\pi^*$  intraligand transitions. In contrast, larger changes in the CD signal were seen in the region of absorption of DNA, which is possibly due to a combination of conformational changes of the DNA induced by the bound complex, or alternatively due to ICD transitions of the bound complexes themselves. These changes can be clearly seen in the difference spectra shown in Fig. 8b. The CD spectra obtained for **Ru-2Nap** revealed significant changes below 300 nm in the region where DNA absorbs. Interestingly, weaker signals were observed in the naphthalimide and the MLCT region, which suggests that the two complexes bind differently to DNA (see Fig. S14 ESI†).

In an attempt to understand in greater detail the different binding modes involved, linear dichroism (LD) measurements were also performed on **Ru·Nap** and **Ru-2Nap** in the presence of DNA. Using this technique intercalative binding gives rise to absorption minima, while groove binding interactions tends to result in absorption maxima. The LD spectra of **Ru·Nap** in the presence of DNA are shown in Fig. 8c. The DNA bands exhibit the characteristic absorption minima below 300 nm. In addition, an absorbance minimum is found in the region of the 1,8-naphthalimide at 350 nm. This suggests a perpendicular orientation of the naphthalimide chromophore relative to the bases (*i.e.* intercalated between the bases). Significantly, the MLCT absorption region possesses structured bands with an absorbance minimum at 420 nm and a maximum at 475 nm. The presence of this structure indicates that the metal complex is closely associated with the DNA with interactions in the groove and possible partial intercalation. These results support our finding above that both components (naphthalimide and  $\text{Ru}(\text{II})$  polypyridyl) are contributing to the overall binding interaction with DNA, and that the  $\text{Ru}(\text{II})$  complex is tightly bound.

In contrast to these results, the LD spectra obtained for **Ru-2Nap** in the presence of DNA contained significantly less structure, see Fig. 8d. This is somewhat surprising giving that the UV-vis and emission titrations demonstrated that **Ru-2Nap** has higher binding affinity for DNA. The LD showed a weakly absorbing minimum in the region of 1,8-naphthalimide absorption at 365 nm. This may be explained by the overlap of the absorbance of the two naphthalimide with different binding modes. If multiple binding interactions occur with DNA, for example where only one naphthalimide is bound to the DNA by intercalation and the other binds *via* a different mode *e.g.* groove binding, the overlap of the negative LD signal of the intercalating and positive signal of the groove binding naphthalimides would be expected to reduce the observed LD signal. The presence of a negative LD signal does, however, suggest that at least one naphthalimide moiety is binding *via* an intercalative mode of binding.

Significantly, no LD signal was observed in the MLCT region of the spectrum for **Ru-2Nap**. Indeed, both CD and LD reveal increased optical activity in the MLCT region of the spectrum for **Ru·Nap** compared to the **Ru-2Nap**. We speculate that there are two possible origins for this observation. Firstly, that the binding of the second naphthalimide causes the posi-

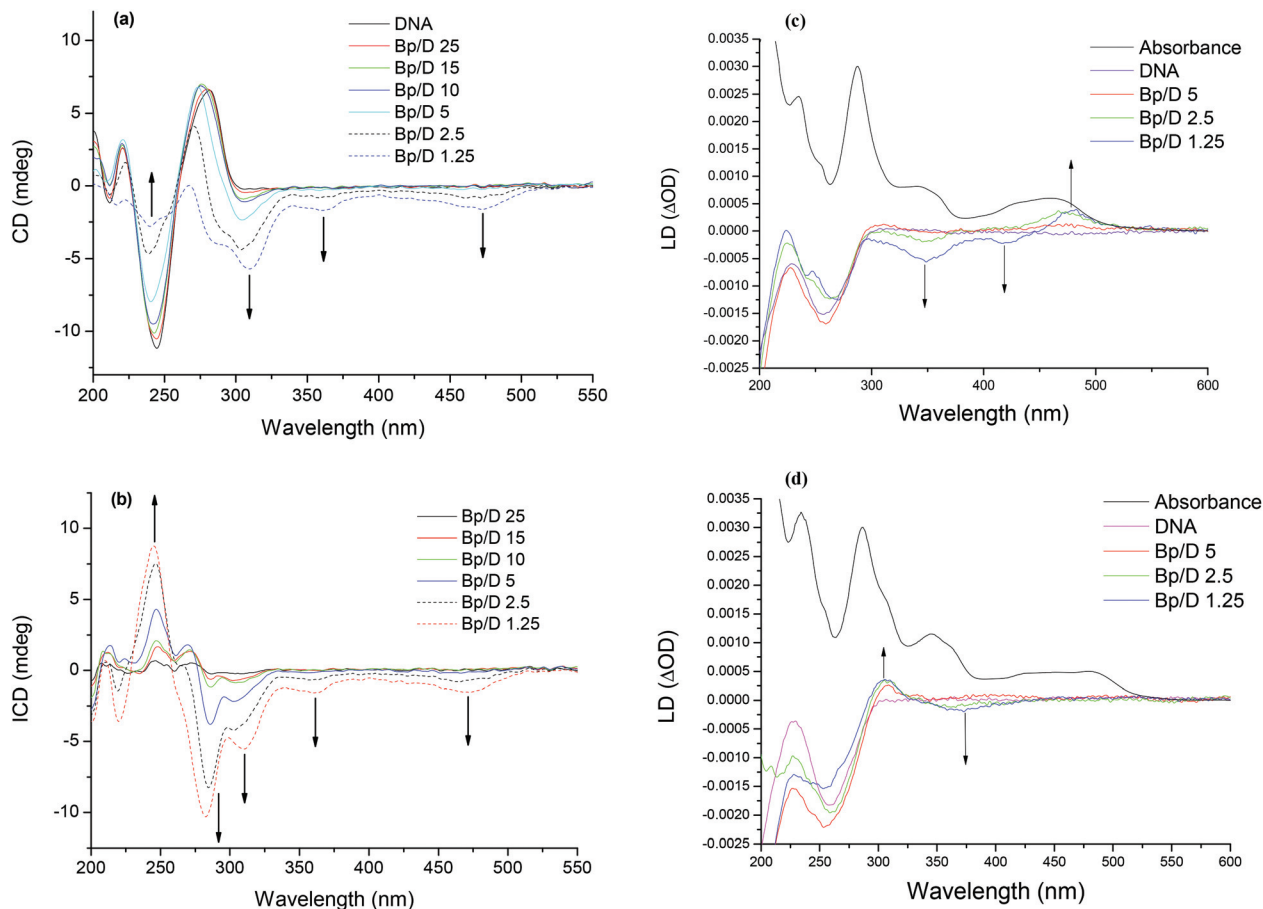


**Fig. 8** Circular dichroism curves of (a) st-DNA (150  $\mu\text{M}$ ) in 10 mM phosphate buffer, at pH 7 in the absence and presence of Ru-Nap at varying ratios and (b) the difference spectra obtained. Linear dichroism curves of st-DNA (150  $\mu\text{M}$ ) in 10 mM phosphate buffer, at pH 7.4 in the absence and presence of (c) Ru-Nap at varying ratios and (d) Ru-2Nap at varying ratios.

tion and orientation of the metal complex change significantly. Secondly, as noted for the naphthalimide signal, the presence of multiple binding orientations may result in overlapping signals from groove binding and intercalating contacts. This second observation would be consistent with strong changes observed for the complex in the MLCT region in the UV-visible absorption titration (Fig. 4b). In summary, such behaviour supports the observations from both CD and  $T_m$  measurements above, where such differing changes were attributed to the fact that Ru-Nap is most likely bound by a classical intercalative mode, whereas Ru-2Nap likely binds in a more complicated and possibly multimodal manner. The ground and excited state DNA binding results and the differences seen in the LD titrations for Ru-Nap and Ru-2Nap clearly demonstrate that while strong binding can be achieved using two naphthalimides, the second naphthalimide moiety can also influence the binding mode of the Ru(II) centre itself with DNA. Such a phenomenon has not, to the best of our knowledge, been demonstrated before using Ru(II)-polypyridyl complexes, flanked with two identical binding ligands such as the naphthalimide units in Ru-2Nap. This is a feature that can have the potential to modulate or tune the ability of such Ru(II)-polypyridyl com-

plexes to interact with DNA, such as their ability to cleave or damage DNA either in the dark or upon light activation. With this in mind we set out to probe these potential effects further using both Ru-Nap and Ru-2Nap.

#### Photocleavage of DNA by Ru-Nap and Ru-2Nap

The ability of Ru-Nap and Ru-2Nap to cleave pBR322 plasmid DNA was investigated and compared to that of Ru(bpy)<sub>3</sub><sup>2+</sup>, see Fig. 9. The amounts of Form I vs. Form II present are detailed in Table S1 ESI,<sup>†</sup> as determined from densitometry measure-

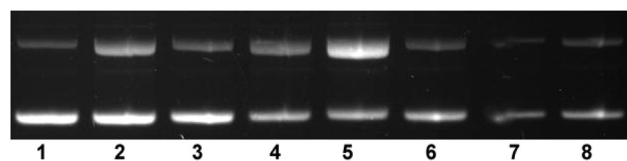


**Fig. 9** Agarose gel electrophoresis of pBR322 DNA (1 mg  $\text{mL}^{-1}$ ) after irradiation at  $\lambda > 390$  nm in 10 mM phosphate buffer, pH 7. Lane 1: Plasmid DNA control; Lane 2: Ru(bpy)<sub>3</sub><sup>2+</sup> (Bp/D 5) 5 min irradiation; Lanes 3–5: Ru-Nap (Bp/D 5) 1, 3, 5 min respectively; Lanes 6–8: Ru-2Nap (Bp/D 5) 1, 3, 5 min respectively.

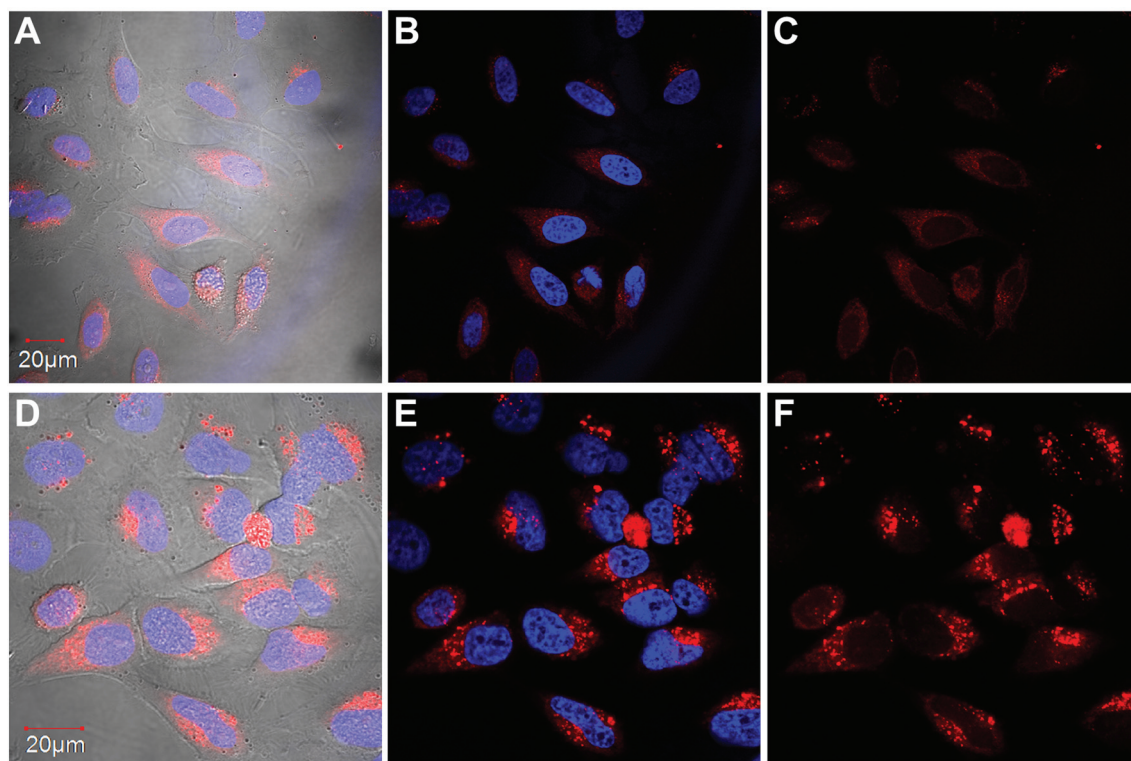


**Fig. 10** Confocal laser scanning microscopy live cell images of **Ru-Nap** (30  $\mu\text{M}$ ) with HeLa cells. Shown are the images obtained with (A) the bright field view of treated cells after 4 h incubation, stained with DAPI (blue) and **Ru-Nap** (red), (B) overlay of **Ru-Nap** (red) and nuclear co-stain DAPI (blue), (C) **Ru-Nap** fluorescence alone (red), (D) the bright field view of treated cells after 24 h incubation, stained with DAPI (blue) and **Ru-Nap** (red), (E) overlay of **Ru-Nap** (red) and nuclear co-stain DAPI (blue), (F) **Ru-Nap** emission alone (red). Compounds were excited by a 488 nm argon laser, emission 600–700 nm. DAPI was excited by a 405 nm diode laser, emission 410–450 nm.

ments of the relative fluorescence intensity of the resulting bands, that were compared to the control photocleaver  $\text{Ru}(\text{bpy})_3^{2+}$ , which was used to evaluate the relative efficiency of cleavage of the conjugate systems. The presence of  $\text{Ru}(\text{bpy})_3^{2+}$  resulted in an increase in **Form II** after 5 minutes irradiation. In the presence of **Ru-Nap** (Lane 3) a small amount of damage was also apparent after only 1 min of irradiation, the percentage of **Form II** having increased to 35%. After 3 minutes irradiation, this had increased to 49% **Form II**, and at the longest irradiation time of 5 minutes had increased to 61% **Form II**. From these results, it can be concluded that **Ru-Nap** displayed a reasonably efficient photocleavage of DNA, leading to more pronounced changes than the reference  $\text{Ru}(\text{bpy})_3^{2+}$ .

In contrast, complex **Ru-2Nap** resulted in only a minor cleavage of the nucleic acid, with **Form I** being the predominant DNA species present, even after 5 minutes irradiation. The different photocleaving ability exhibited by the two complexes is attributed to their different DNA binding modes which position the  $\text{Ru}(\text{II})$ -polypyridyl centre in different environments. A reduction in activity is likely to be due to the proximity of

the metal complex to the DNA. This could arise if the complex was poorly positioned or held away from the DNA bases. On the other hand, if the complex is very tightly associated with the DNA groove structure, then access to molecular oxygen and the photoreactivity would be reduced. This may be the case for **Ru-2Nap**. This is a somewhat unexpected result as it demonstrates that the ‘cooperativity’ that results in increasing binding affinity can have major and ‘negative’ secondary effects. Which, as stated above, we believe to be a direct consequence of the positioning of  $\text{Ru}(\text{II})$ -polypyridyl centre along the DNA backbone when the second naphthalimide unit is bound.

#### Cellular uptake, localisation and viability studies

With the aim of using **Ru-Nap** and **Ru-2Nap** as dual functioning imaging and therapeutic agents, their ability to be internalised in target cells is of vital importance. In order to evaluate the ability of **Ru-Nap** and **Ru-2Nap** to localise within cells, fluorescence confocal microscopy and cell viability analyses were undertaken. Confocal microscopy was carried out in order to provide visual evidence of the localisation of **Ru-Nap** and **Ru-2Nap** in HeLa cervical cancer cells. Populations of live cells ( $0.5 \times 10^5$ ) were incubated with both complexes (30  $\mu\text{M}$ ) at 37  $^\circ\text{C}$  for 4 and 24 h before being treated with the fluorescent nuclear stain DAPI and viewed using an Olympus FV1000

§ Determination of the relative intensity of the bands showed that DNA was somewhat damaged to begin with, being comprised of 73% **Form I** and 27% **Form II**.



**Table 3** The effects of **Ru-Nap** and **Ru-2Nap** on HeLa cells with or without light activation as determined using an AlamarBlue viability assay

IC <sub>50</sub> value (μM)	Dark	Light activation
<b>Ru-Nap</b>	29.8	7.81
<b>Ru-2Nap</b>	>30	>30

point scanning microscope with a 60× oil immersion lens. The results obtained are exemplified in Fig. 10, which shows the fluorescence confocal laser scanning microscopy images of live HeLa cells after incubation with **Ru-Nap** for 4 and 24 h (the corresponding images for **Ru-2Nap** are shown in Fig. S15 ESI†). The observed images show the presence of red luminescence emanating from within the cells' interior, associated around the nucleus. Although we do not demonstrate co-localisation with any specific organelles for this study, our previous work in this area<sup>32,54</sup> has demonstrated that related Ru(II) complexes localise predominantly within the mitochondria, leading to perinuclear clustering, with some localisation observed in the lysosomes and the endoplasmic reticulum. Similar localisation results has been seen by several other researchers.<sup>4a,12a</sup> Additionally, cellular viability was measured using an AlamarBlue assay. Results showed a significant reduction in IC<sub>50</sub> values following light activation with compound **Ru-Nap**, compared to cells maintained in the dark (7.8 μM *versus* 30 μM). In contrast, for compound **Ru-2Nap**, there was no difference between light and dark IC<sub>50</sub> values, with the cells showing only a small degree of toxicity at the highest concentration tested, 30 μM, see Table 3. The production of reactive oxygen species (ROS) may be a potential mechanism through which these novel compounds induce apoptosis.<sup>54</sup> Taken together, these results are of considerable significance in providing evidence for our assertion that the use of such bifunctional complexes, comprising separate hydrophilic and hydrophobic centres is a viable means of effecting cellular accumulation of Ru(II) based probes and reactive agents within cells for potential diagnostic and therapeutic use.

## Conclusions

In conclusion, we have reported the preparation of two new DNA binding ruthenium complexes appended with one (**Ru-Nap**), or two (**Ru-2Nap**) naphthalimides through flexible alkyl chain linkers, and investigated their photophysical and biological properties. The luminescence of the complexes is found to be solely MLCT based with excitation of the naphthalimide centres resulting in MLCT emission, as evidenced from their excitation spectra. This presents the opportunity to obtain MLCT-based emission from both complexes through excitation into either the MLCT or the naphthalimide absorption bands. These complexes were found to bind strongly to DNA; demonstrating that our design supports cooperativity,

where the naphthalimide moiety greatly assists in inducing strong association with DNA by displaying large changes in the steady state absorption and emission of both complexes. Both complexes were also shown to exhibit CD activity in the presence of DNA further confirming their ability to bind strongly to DNA. The binding mode of these complexes with DNA was further investigated by observing the changes in the LD spectra. From the relatively large negative band in the LD spectrum when bound to DNA, **Ru-Nap** appeared to bind to DNA *via* intercalation of the naphthalimide moiety; this being further supported by a large  $\Delta T_m$ . In contrast, **Ru-2Nap** was shown to bind to DNA in a more complex fashion; this being evident from the small LD signal of the naphthalimide moiety when bound to DNA and a small  $\Delta T_m$ . This is an extremely important result as it clearly demonstrates that a strong association with the DNA is maintained between the naphthalimide and the Ru(II)-polypyridyl unit in the case of **Ru-Nap**. However, in the case of **Ru-2Nap**, the picture is more complicated, as here, both the naphthalimide units are bound to DNA causing a change in the position of the Ru(II)-polypyridyl centre at the DNA backbone. The result of this change in binding manifests in the difference in photoreactivity between the two complexes in the presence of DNA. Upon light activation **Ru-Nap** was shown to effectively cleave plasmid DNA while **Ru-2Nap** showed poor cleavage. Moreover, this difference in photoreactivity *in vitro* was also observed *in cellulo*. While both complexes are readily taken up by HeLa cells and emission from both complexes was observed within the cells after 4 hours incubation (the complexes were observed to cluster next to the nucleus), **Ru-Nap** was found to reduce HeLa cell viability upon photoactivation, whereas **Ru-2Nap** was nontoxic under identical conditions. The results presented herein demonstrate different activity observed for two closely related conjugates **Ru-Nap** and **Ru-2Nap**, where the structural difference is the presence of a second naphthalimide unit in **Ru-2Nap**, does lead to cooperativity in DNA binding. Such modification however, can have a detrimental effect on their biological activity when such structures are considered as potential therapeutic agents. To the best of our knowledge this has not previously been observed or postulated for such systems when designing DNA targeting and responsive therapeutics. Such properties are highly desirable when one considers the applications of such structures as imaging agents for use in molecular biology, as **Ru-2Nap** is not particularly toxic upon light irradiation. Hence, while **Ru-Nap** is a potential candidate for use in therapy, **Ru-2Nap**, is a potential candidate for use in fluorescence imaging. We are currently investigating this and such functions of other Ru(II) based polypyridyl complexes in greater detail.

## Experimental

### Materials and instrumentation

All reagents and solvents were purchased commercially and used without further purification unless otherwise stated.

Anhydrous solvents were prepared using standard procedures, according to Vögel, with distillation under argon prior to each use. Solutions of DNA in 10 mM phosphate buffer (pH 7) gave a ratio of UV absorbance at 260 and 280 nm of 1.86 : 1, indicating that the DNA was sufficiently free of protein. Its concentration was determined spectrophotometrically using the molar absorptivity of  $6600 \text{ M}^{-1} \text{ cm}^{-1}$  (260 nm).

All NMR spectra were recorded using a Bruker DPX-400 Avance spectrometer, operating at 400.13 MHz for  $^1\text{H}$  NMR and 100.6 MHz for  $^{13}\text{C}$  NMR, or a Bruker AV-600 spectrometer, operating at 600.1 MHz for  $^1\text{H}$  NMR and 150.2 MHz for  $^{13}\text{C}$  NMR. Shifts are referenced relative to the internal solvent signals. Electrospray mass spectra were recorded on a Micro-mass LCT spectrometer, running Mass Lynx NT V 3.4 on a Waters 600 controller connected to a 996 photodiode array detector with HPLC-grade methanol or acetonitrile. High resolution mass spectra were determined by a peak matching method, using leucine Enkephalin, (Tyr-Gly-Gly-Phe-Leu), as the standard reference ( $m/z = 556.2771$ ). Melting points were determined using an IA9000 digital melting point apparatus. Infrared spectra were recorded on a Perkin Elmer Spectrum One FT-IR spectrometer fitted with a Universal ATR Sampling Accessory. Elemental analysis was conducted at the Micro-analytical Laboratory, School of Chemistry and Chemical Biology, University College Dublin.

UV-visible absorption spectra were recorded on a Varian Cary 50 spectrometer. Emission spectra were recorded on a Cary Eclipse Luminescence spectrometer. The luminescence quantum yields were calculated by comparison with  $[\text{Ru}(\text{bpy})_3]^{2+}$ . Circular dichroism (CD) spectra were recorded at a concentration corresponding to an optical density of approximately 1.0, in buffered solutions, on a Jasco J-810-150S spectropolarimeter.

### Biological investigations

**Cell culture.** HeLa cells were grown in Dulbecco's Modified Eagle Medium supplemented with 10% fetal bovine serum and  $50 \mu\text{g}$  per ml penicillin/streptomycin at  $37^\circ\text{C}$  in a humidified atmosphere of 5%  $\text{CO}_2$ .

**Viability assay.**  $5 \times 10^3$  cells per well were seeded in a 96-well plate and treated with the respective compound for 24 h + irradiation with  $18 \text{ J cm}^{-2}$  of light using a Hamamatsu L2570 200 Watt HgXe Arc Lamp equipped with a NaNO<sub>2</sub> filter for 60 min. After 24 h, each well was then treated with  $20 \mu\text{l}$  of Alamar Blue (BioSource) (pre-warmed to  $37^\circ\text{C}$ ) and left to incubate at  $37^\circ\text{C}$  in the dark for 4–6 h. Fluorescence was read using at 590 nm (excitation 544 nm). The control untreated cells represented 100% cell viability. All data points (expressed as means  $\pm$  S.E.M.) were analysed using GRAPHPAD Prism (version 4) software (Graphpad software Inc., San Diego, CA).

**Confocal microscopy.** HeLa cells were seeded at a density of  $1 \times 10^5$  cells per 2 ml, left for 24 h before the required treatment. Cells were then washed twice, stained with and analysed by live confocal microscopy using an Olympus FV1000 point scanning microscope with a  $60\times$  oil immersion lens with an NA (numerical aperture) of 1.42. The software used to collect

images was FluoView Version 7.1 software. Compounds were excited by a 488 nm argon laser, emission 600–700 nm. DAPI was excited by a 405 nm diode laser, emission 410–450 nm.

***N*-[(*tert*-Butoxycarbonyl)-5-aminopentyl]-1,8-naphthalimide (1).** 1,8-Naphthalic anhydride (0.80 g, 4.04 mmol, 1 eq.), *N*-(*tert*-butoxycarbonyl)-1,5-diaminopentane (0.90 g, 4.45 mmol, 1.1 eq.), and  $\text{Et}_3\text{N}$  (1.23 g, 1.69 ml, 12.12 mmol, 3 eq.) were added to anhydrous toluene (60 ml) and the mixture heated at reflux for 24 h. The mixture was filtered hot through celite and concentrated under vacuum. The residue was dissolved in  $\text{CH}_2\text{Cl}_2$  (100 ml), washed with 0.1 M HCl ( $2 \times 20 \text{ ml}$ ), water (20 ml), dried over  $\text{MgSO}_4$  and concentrated under vacuum. The product was obtained as an orange oily solid without need for further purification (0.57 g, 82%).  $^1\text{H}$  NMR ( $\text{DMSO}[D_6]$ , 400 MHz,  $\delta$ ) 8.53 (2H, d,  $J = 7.6 \text{ Hz}$ ), 8.49 (2H, d,  $J = 8.5 \text{ Hz}$ ), 7.91 (2H, m), 6.82 (1H, s), 4.07 (2H, t,  $J = 7.0 \text{ Hz}$ ), 2.94 (2H, d,  $J = 6.0 \text{ Hz}$ ), 1.65 (2H, m), 1.40 (13H, m);  $^{13}\text{C}$  NMR ( $\text{DMSO}[D_6]$ , 100 MHz,  $\delta$ ) 163.4, 155.6, 134.3, 131.3, 130.7, 127.4, 122.1, 77.3, 54.9, 50.8, 29.2, 28.2, 27.3, 23.8; ESI-MS  $m/z$  405.1809 ( $\text{M} + \text{Na}$ )<sup>+</sup>; IR (ATR,  $\text{cm}^{-1}$ ): 1698 (m,  $-\text{CO}-\text{N}-\text{CO}-$ ), 1656 (s,  $-\text{CONH}-$ )

***N*-(Pentylammonium)-1,8-naphthalimide trifluoroacetate (2).** Compound 1 (0.88 g, 2.29 mmol, 1 eq.) was stirred in TFA (15 ml) for 1 h at room temperature. The TFA was removed under vacuum and co-evaporated several times with  $\text{CH}_2\text{Cl}_2$ . After drying under high vacuum the solid was obtained as a pale brown solid (0.90 g, 99%).  $^1\text{H}$  NMR ( $\text{CD}_3\text{OD}$ , 400 MHz,  $\delta$ ) 8.30 (2H, d,  $J = 7.6 \text{ Hz}$ ), 8.11 (2H, d,  $J = 8.0 \text{ Hz}$ ), 7.62 (2H, t,  $J = 7.5 \text{ Hz}$ ), 4.04 (2H, m), 2.97 (2H, m), 1.74 (4H, m), 1.48 (2H, m);  $^{13}\text{C}$  NMR ( $\text{CD}_3\text{OD}$ , 100 MHz,  $\delta$ ) 163.8, 133.8, 113.2130.3, 127.2, 126.3, 121.5, 39.0, 38.8, 26.6, 26.3, 23.0; ESI-MS  $m/z$  283.1456 ( $\text{M}$ )<sup>+</sup>; IR (ATR,  $\text{cm}^{-1}$ ): 3179 (w,  $-\text{NH}_2$ ), 1694 (m,  $-\text{CO}-\text{N}-\text{CO}-$ ); m.p. 151–152  $^\circ\text{C}$ .

**4-[*N*-(Pentylcarboxamide)-1,8-naphthalimide]-4'-methyl-2,2'-bipyridine (3a).** Compound 2 (0.15 g, 0.38 mmol, 1.1 eq.) and  $\text{Et}_3\text{N}$  (0.10 g, 0.14 ml, 1.02 mmol, 3 eq.) were dissolved in dry  $\text{CH}_2\text{Cl}_2$  and 4-(carbonylchloride)-4'-methyl-2,2'-bipyridine (0.08 g, 0.34 mmol, 1 eq.) dissolved in dry  $\text{CH}_2\text{Cl}_2$ , was added dropwise. The solvent was removed under reduced pressure. The resulting residue was stirred with 0.1 M HCl, filtered and washed with water. Purification was performed by silica column chromatography eluting with  $\text{CH}_2\text{Cl}_2/\text{MeOH}$  10% the product was obtained as a pale brown solid (0.14 g, 83%); calculated for  $\text{C}_{29}\text{H}_{26}\text{N}_4\text{O}_3 \cdot 0.25\text{CH}_2\text{Cl}_2$ : C, 70.29; H, 5.34; N, 11.21. Found: C, 70.62; H, 5.48; N, 10.84;  $^1\text{H}$  NMR ( $\text{DMSO}[D_6]$ , 400 MHz,  $\delta$ ): 8.90 (1H, m,  $\text{NH}$ ), 8.76 (1H, d,  $J = 5.0 \text{ Hz}$ ,  $\text{Bpy-H}$ ), 8.71 (1H, s,  $\text{Bpy-H}$ ), 8.57 (1H, d,  $J = 5.0 \text{ Hz}$ ,  $\text{Bpy-H}$ ), 8.48 (2H, d,  $J = 7.0 \text{ Hz}$ ,  $\text{Naph-H}$ ), 8.44 (2H, d,  $J = 8.0 \text{ Hz}$ ,  $\text{Naph-H}$ ), 8.26 (1H, s,  $\text{Bpy-H}$ ), 7.85 (2H, m,  $\text{Naph-H}$ ), 7.73 (1H, dd,  $J = 1.5, 5.0 \text{ Hz}$ ,  $\text{Bpy-H}$ ), 7.33 (1H, d,  $J = 4.5 \text{ Hz}$ ,  $\text{Bpy-H}$ ), 4.07 (2H, t,  $J = 7.6 \text{ Hz}$ ,  $\text{CH}_2$ ), 3.29 (2H, m,  $\text{CH}_2$ ), 2.44 (3H, s,  $\text{CH}_3$ ), 1.71 (2H, m,  $\text{CH}_2$ ), 1.63 (2H, m,  $\text{CH}_2$ ), 1.41 (2H, m,  $\text{CH}_2$ ); IR (ATR,  $\text{cm}^{-1}$ ): 1698 (m,  $-\text{CO}-\text{N}-\text{CO}-$ ), 1658 (s,  $-\text{CONH}-$ ); m.p. 162–164  $^\circ\text{C}$ .

**4,4'-Bis-[(*N*-pentylcarboxamide)-1,8-naphthalimide]-2,2'-bipyridine (3b).** Was prepared as above with compound 2

(0.40 g, 1.01 mmol, 2.1 eq.) and 4,4'-bis(carbonylchloride)-2,2'-bipyridine (0.14 g, 0.48 mmol, 1 eq.). The product was obtained as a purple solid (0.35 g, 95%).  $^1\text{H}$  NMR (DMSO- $d_6$ ], 400 MHz,  $\delta$ ) 8.97 (1H, br s, NH), 8.80 (1H, m, Bpy-H), 8.75 (1H, m, Bpy-H), 8.46 (2H, d,  $J = 7.0$  Hz, Naph-H), 8.42 (2H, d,  $J = 8.0$  Hz, Naph-H), 7.83 (2H, m, Naph-H), 7.77 (1H, m, Bpy-H), 4.06 (2H, m, CH<sub>2</sub>),  $\sim 3.30$  (CH<sub>2</sub>, under solvent peak – from CH COSY), 1.69 (2H, m, CH<sub>2</sub>), 1.63 (2H, m, CH<sub>2</sub>), 1.41 (2H, m, CH<sub>2</sub>);  $^{13}\text{C}$  NMR (DMSO- $d_6$ ], 150 MHz,  $\delta$ ) 164.8, 163.7, 155.8, 150.2, 143.3, 134.5, 131.6, 131.0, 127.7, 127.5, 122.4, 122.2, 118.5, 40.1, 39.7, 28.9, 27.6, 24.3; IR (ATR, cm<sup>-1</sup>): 1698 (w, –CO–N–CO–), 1658 (m, –CONH–); m.p 210–211 °C.

**RuNap.** Compound **3a** (0.09 g, 0.19 mmol, 1 eq.) and Ru(bpy)<sub>2</sub>Cl<sub>2</sub>·2H<sub>2</sub>O (0.12 g, 0.23 mmol, 1.2 eq.) were suspended in DMF/H<sub>2</sub>O (20 ml) and the solution degassed by bubbling with Argon for 10 min. The reaction mixture was heated at reflux under an Argon atmosphere for 20 h. The solvent was removed under vacuum. The residue was dissolved in water and filtered. To the filtrate was added a concentrated aqueous solution of NH<sub>4</sub>PF<sub>6</sub>, and the resulting precipitate extracted into CH<sub>2</sub>Cl<sub>2</sub>. The product was purified by silica flash column chromatography eluting with CH<sub>3</sub>CN/H<sub>2</sub>O/NaNO<sub>3</sub>(sat) 40 : 4 : 1. The chloride salt of the complex was reformed by stirring a solution of the complex in MeOH with Amberlite ion exchange resin (Cl<sup>-</sup> form). The chloride salt was further purified by column chromatography on Sephadex LH-20 eluting with methanol giving them product as a red/brown solid (0.16 g, 86%). Calculated for C<sub>49</sub>H<sub>42</sub>F<sub>12</sub>N<sub>8</sub>O<sub>3</sub>P<sub>2</sub>Ru·CH<sub>3</sub>CN: C, 50.09; H, 3.71; N, 10.31. Found: C, 50.38; H, 3.43; N, 10.39% accurate MS ( $m/z$ ) calculated for C<sub>49</sub>H<sub>42</sub>N<sub>8</sub>O<sub>3</sub>Ru (M<sup>2+</sup>): 892.2423. Found 892.2420;  $^1\text{H}$  NMR (CD<sub>3</sub>CN, 400 MHz,  $\delta$ ): 8.90 (1H, d,  $J = 1.5$  Hz), 8.60 (1H, s), 8.51 (6H, m), 8.34 (2H, d,  $J = 7.5$  Hz), 8.08 (4H, m), 7.82 (2H, m), 7.76 (6H, m), 7.63 (1H, dd,  $J = 1.5$ , 6.0 Hz), 7.57 (2H, d,  $J = 6.0$  Hz), 7.40 (4H, m), 7.29 (1H, d,  $J = 5.5$  Hz), 4.13 (2H, t,  $J = 7.5$  Hz), 3.43 (2H, m), 2.56 (3H, s), 1.74 (4H, m), 1.49 (2H, m);  $^{13}\text{C}$  NMR (CD<sub>3</sub>CN, 150 MHz,  $\delta$ ): 163.9, 162.9, 157.8, 156.9, 156.84, 156.80, 156.7, 156.0, 152.1, 151.6, 151.5, 151.4, 150.6, 142.7, 137.7, 133.9, 131.6, 130.5, 128.5, 127.9, 127.5, 126.9, 125.5, 124.4, 124.2, 124.1, 122.7, 121.5, 39.7, 39.6, 28.5, 27.3, 24.0, 20.1; IR (ATR, cm<sup>-1</sup>): 1698 (m, –CO–N–CO–), 1658 (m, –CONH–).

**Ru-2Nap.** Was prepared as above, using (0.115 g, 0.15 mmol, 1 eq.) of compound **3b** and (0.085 g, 0.16 mmol, 1.1 eq.) Ru(bpy)<sub>2</sub>Cl<sub>2</sub>·2H<sub>2</sub>O. Product as a red/brown solid (0.142 g, 76%). Found C, 51.94; H, 3.81; N, 8.92% C<sub>66</sub>H<sub>56</sub>F<sub>12</sub>N<sub>10</sub>O<sub>6</sub>P<sub>2</sub>Ru·3H<sub>2</sub>O requires C, 51.80; H, 4.08; N, 9.15%;  $^1\text{H}$  NMR (CD<sub>3</sub>OD, 400 MHz,  $\delta$ ) 9.34 (1H, s), 8.76 (2H, dd,  $J = 3.0$ , 8.0 Hz), 8.33 (2H, d,  $J = 7.0$  Hz), 8.18 (4H, m), 8.02 (1H, d,  $J = 5.5$  Hz), 7.86 (3H, m), 7.64 (2H, m), 7.54 (2H, pent,  $J = 6.5$  Hz), 4.06 (2H, t,  $J = 7.6$  Hz), 3.45 (2H, m), 1.73 (4H, m), 1.49 (2H, m);  $^{13}\text{C}$  NMR (CD<sub>3</sub>OD, 100 MHz,  $\delta$ ) 164.44, 164.39, 158.0, 157.4, 157.3, 152.4, 151.8, 151.6, 143.2, 138.6, 134.4, 131.9, 130.9, 128.13, 128.1, 128.0, 127.0, 125.8, 124.8, 122.5, 122.4, 40.2, 40.1, 28.9, 27.7, 24.5; ESI-MS  $m/z$  1186.3412 (M)<sup>+</sup>; IR (ATR, cm<sup>-1</sup>): 1695 (m, –CO–N–CO–), 1652 (s, –CONH–).

## Acknowledgements

We are grateful to Trinity College Dublin, Science Foundation Ireland, for SFI 2010 PI (09/RFP/CHS2516), 2013 PI (10/IN.1/B2999) awards and RFP 2009 (09/RFP/CHS2516) awards, Irish Research Council (IRC) and Irish Research Council for Sciences, Engineering and Technology (IRCSET) (postgraduate studentship to G. J. Ryan, R. B. P. Elmes and F. E. Poynton), Sardinian Programma Master and Back Scheme (postgraduates studentship for M-L Erby) and HEA PRTL Cycle 3 and 4 for financial support. We particularly would like to thank Prof. John M. Kelly and Dr Sandra Bright for valuable discussions and support during this project.

## Notes and references

- (a) N. Hadjiliadis and E. Sletten, *Metal Complex - DNA Interactions*, Wiley-Blackwell, UK, 2009; (b) *Bioinorganic Medicinal Chemistry*, ed. E. Alessio, Wiley-VCH Verlag GmbH & Co., Germany, 2011; (c) P. C. A. Bruijninx and P. J. Sadler, *Curr. Opin. Chem. Biol.*, 2008, **12**, 197–206; (d) C. X. Zhang and S. J. Lippard, *Curr. Opin. Chem. Biol.*, 2003, **7**, 481–489; (e) Q. Zhao, C. Huang and F. Li, *Chem. Soc. Rev.*, 2011, **40**, 2508.
- (a) C. Moucheron, A. Kirsch-De Mesmaeker and J. Kelly, in *Less Common Metals in Proteins and Nucleic Acid Probes*, Springer, Berlin Heidelberg, 1998, **92**, 163–216; (b) K. E. Erkkila, D. T. Odom and J. K. Barton, *Chem. Rev.*, 1999, **99**, 2777–2796; (c) A. W. McKinley, P. Lincoln and E. M. Tuite, *Coord. Chem. Rev.*, 2011, **255**, 2676.
- (a) N. A. P. Kane-Maguire and J. F. Wheeler, *Coord. Chem. Rev.*, 2001, **211**, 145–162; (b) S. Vasudevan, J. A. Smith, M. Wojdyla, T. McCabe, N. C. Fletcher, S. J. Quinn and J. M. Kelly, *Dalton Trans.*, 2010, **39**, 3990–3998.
- (a) M. R. Gill and J. A. Thomas, *Chem. Soc. Rev.*, 2012, **41**, 3179–3192; (b) C. Metcalfe and J. A. Thomas, *Chem. Soc. Rev.*, 2003, **32**, 215–224.
- A. Mihailovic, I. Vladescu, M. McCauley, E. Ly, M. C. Williams, E. M. Spain and M. E. Nuñez, *Langmuir*, 2006, **22**, 4699–4709.
- (a) T. C. Jenkins, *Curr. Med. Chem.*, 2000, **7**, 99–115; (b) M. J. Hannon, *Chem. Soc. Rev.*, 2007, **36**, 280–295.
- (a) R. Zhao, R. Hammit, R. P. Thummel, Y. Liu, C. Turro and R. M. Snapka, *Dalton Trans.*, 2009, 10926–10931; (b) Q. Yu, Y. Liu, L. Xu, C. Zheng, F. Le, X. Qin, Y. Liu and J. Liu, *Eur. J. Med. Chem.*, 2014, **82**, 82–95; (c) K. J. Kilpin, C. M. Clavel, F. Edefe and P. J. Dyson, *Organometallics*, 2012, **31**, 7031; (d) S. Ding, X. Qiao, J. Suryadi, G. S. Marrs, G. L. Kucera and U. Bierbach, *Angew. Chem., Int. Ed.*, 2013, **52**, 3350; (e) A. J. Pickard, F. Liu, T. F. Bartenstein, L. G. Haines, K. E. Levine, G. L. Kucera and U. Bierbach, *Chem. – Eur. J.*, 2014, **20**, 16174.
- D. B. Hall, R. E. Holmlin and J. K. Barton, *Nature*, 1996, **382**, 731–735.

- 9 C. Moucheron, A. Kirsch-De Mesmaeker and J. M. Kelly, *J. Photochem. Photobiol., B*, 1997, **40**, 91–106.
- 10 S. Neidle and M. Waring, *Molecular Aspects of Anticancer Drug DNA Interactions*, Taylor & Francis, Boca Roca, 1994.
- 11 (a) M. R. Gill, J. Garcia-Lara, S. J. Foster, C. Smythe, G. Battaglia and J. A. Thomas, *Nat. Chem.*, 2009, **1**, 662–667; (b) M. R. Gill, H. Derrat, C. G. W. Smythe, G. Battaglia and J. A. Thomas, *ChemBioChem*, 2011, **12**, 877.
- 12 (a) M. R. Gill, D. Cecchin, M. G. Walker, R. S. Mulla, G. Battaglia, C. Smythe and J. A. Thomas, *Chem. Sci.*, 2013, **4**, 4512–4519; (b) C. A. Puckett and J. K. Barton, *Biochemistry*, 2008, **47**, 11711–11716; (c) L. Cosgrave, M. Devocelle, R. J. Forster and T. E. Keyes, *Chem. Commun.*, 2010, **46**, 103; (d) F. R. Svensson, M. Matson, M. Li and P. Lincoln, *Biophys. Chem.*, 2010, **149**, 102.
- 13 (a) R. Martinez and L. Chacon-Garcia, *Curr. Med. Chem.*, 2005, **12**, 127–151; (b) K. K.-W. Lo, T. K. M. Lee, J. S. Y. Lau, W. L. Poonand and S. H. Cheng, *Inorg. Chem.*, 2008, **47**, 200; (c) H. Komatsu, K. Yoshihara, H. Yamada, Y. Kimura, A. Son, S.-I. Nishimoto and K. Tanabe, *Chem. – Eur. J.*, 2013, **19**, 1971; (d) M. Matson, F. R. Svensson, B. Nordén and P. Lincoln, *J. Phys. Chem. B*, 2011, **115**, 1706.
- 14 A. E. Friedman, J. C. Chambron, J. P. Sauvage, N. J. Turro and J. K. Barton, *J. Am. Chem. Soc.*, 1990, **112**, 4960–4962.
- 15 (a) C. Metcalfe, H. Adams, I. Haq and J. A. Thomas, *Chem. Commun.*, 2003, 1152–1153; (b) Y. Sun, L. E. Joyce, N. M. Dickson and C. Turro, *Chem. Commun.*, 2010, **46**, 2426–2428; (c) C. Tan, S. Wu, S. Lai, M. Wang, Y. Chen, L. Zhou, Y. Zhu, W. Lian, W. Peng, L. Ji and A. Xu, *Dalton Trans.*, 2011, **40**, 8611; (d) F. R. Svensson, M. Li, B. Nordén and P. Lincoln, *J. Phys. Chem. B*, 2008, **112**, 10969.
- 16 (a) I. Ortman, B. Elias, J. M. Kelly, C. Moucheron and A. Kirsch-DeMesmaeker, *Dalton Trans.*, 2004, 668–676; (b) B. Elias, C. Creely, G. W. Doorley, M. M. Feeney, C. Moucheron, A. Kirsch-DeMesmaeker, J. Dyer, D. C. Grills, M. W. George, P. Matousek, A. W. Parker, M. Towrie and J. M. Kelly, *Chem. – Eur. J.*, 2008, **14**, 369–375.
- 17 L. Jacquet, J. M. Kelly and A. K.-D. Mesmaeker, *J. Chem. Soc., Chem. Commun.*, 1995, 913–914.
- 18 J. G. Vos and J. M. Kelly, *Dalton Trans.*, 2006, 4869–4883.
- 19 B. Elias and A. Kirsch-De Mesmaeker, *Coord. Chem. Rev.*, 2006, **250**, 1627–1641.
- 20 R. B. P. Elmes, K. N. Orange, S. M. Cloonan, D. C. Williams and T. Gunnlaugsson, *J. Am. Chem. Soc.*, 2011, **133**, 15862–15865.
- 21 P. B. Dervan and R. W. Bürli, *Curr. Opin. Chem. Biol.*, 1999, **3**, 688–693.
- 22 I. Haq, P. Lincoln, D. Suh, B. Norden, B. Z. Chowdhry and J. B. Chaires, *J. Am. Chem. Soc.*, 1995, **117**, 4788–4796.
- 23 J. P. Hall, K. O'Sullivan, A. Naseer, J. A. Smith, J. M. Kelly and C. J. Cardin, *Proc. Natl. Acad. Sci. U. S. A.*, 2011, **108**, 17610–17614.
- 24 H. Niyazi, J. P. Hall, K. O'Sullivan, G. Winter, T. Sorensen, J. M. Kelly and C. J. Cardin, *Nat. Chem.*, 2012, **4**, 621–628.
- 25 (a) H. Song, J. T. Kaiser and J. K. Barton, *Nat. Chem.*, 2012, **4**, 615–620; (b) S. Neidle, *Nat. Chem.*, 2012, **4**, 594–595.
- 26 (a) A. Ghosh, P. Das, M. R. Gill, P. Kar, M. G. Walker, J. A. Thomas and A. Das, *Chem. – Eur. J.*, 2011, **17**, 2089–2098; (b) X. Tian, M. R. Gill, I. Cant, J. A. Thomas and G. Battaglia, *ChemBioChem*, 2011, **12**, 548–551; (c) T. Wilson, M. P. Williamson and J. A. Thomas, *Org. Biomol. Chem.*, 2010, **8**, 2617–2621.
- 27 J. M. Kelly, A. B. Tossi, D. J. McConnell and C. Ohuigin, *Nucleic Acids Res.*, 1985, **13**, 6017–6034.
- 28 B. M. Zeglis, V. C. Pierre and J. K. Barton, *Chem. Commun.*, 2007, 4565–4579.
- 29 I. Ortman, S. Content, N. Boutonnet, A. Kirsch-De Mesmaeker, W. Bannwarth, J. F. Constant, E. Defrancq and J. Lhomme, *Chem. – Eur. J.*, 1999, **5**, 2712–2721.
- 30 G. J. Ryan, S. Quinn and T. Gunnlaugsson, *Inorg. Chem.*, 2008, **47**, 401–403.
- 31 (a) E. B. Veale, D. O. Frimannsson, M. Lawler and T. Gunnlaugsson, *Org. Lett.*, 2009, **11**, 4040–4043; (b) E. B. Veale and T. Gunnlaugsson, *J. Org. Chem.*, 2010, **75**, 5513–5525; (c) S. Murphy, S. A. Bright, F. E. Poynton, T. McCabe, J. A. Kitchen, E. B. Veale, D. C. Williams and T. Gunnlaugsson, *Org. Biomol. Chem.*, 2014, **12**, 6610–6623.
- 32 R. B. P. Elmes, M. Erby, S. A. Bright, D. C. Williams and T. Gunnlaugsson, *Chem. Commun.*, 2012, **48**, 2588–2590.
- 33 A. M. Nonat, S. J. Quinn and T. Gunnlaugsson, *Inorg. Chem.*, 2009, **48**, 4646–4648.
- 34 S. Banerjee, E. B. Veale, C. M. Phelan, S. A. Murphy, G. M. Tocci, L. J. Gillespie, D. O. Frimannsson, J. M. Kelly and T. Gunnlaugsson, *Chem. Soc. Rev.*, 2013, **42**, 1601–1618.
- 35 (a) S. Banerjee, J. A. Kitchen, T. Gunnlaugsson and J. M. Kelly, *Org. Biomol. Chem.*, 2013, **11**, 5642–5655; (b) S. Banerjee, J. A. Kitchen, T. Gunnlaugsson and J. M. Kelly, *Org. Biomol. Chem.*, 2012, **10**, 3033–3043; (c) S. Banerjee, S. A. Bright, J. A. Smith, J. Burgeat, M. Martinez-Calvo, D. C. Williams, J. M. Kelly and T. Gunnlaugsson, *J. Org. Chem.*, 2014, **79**, 9272–9283.
- 36 Recent examples of the use of 1,8-naphthalimides based probes and sensors in cells: (a) J. Pancholi, D. J. Hodson, K. Jobe, G. A. Rutter, S. M. Goldup and M. Watkinson, *Chem. Sci.*, 2014, **5**, 3528–3535; (b) X. Sun, Q. Xu, G. Kim, S. E. Flower, J. P. Lowe, J. Yoon, J. S. Fossey, X. Qian, S. D. Bull and T. D. James, *Chem. Sci.*, 2014, **5**, 3368–3373; (c) M. H. Lee, B. Yoon, J. S. Kim and J. L. Sessler, *Chem. Sci.*, 2013, **4**, 4121–4126; (d) E. E. Langdon-Jones, N. O. Symonds, S. E. Yates, A. J. Hayes, D. Lloyd, R. Williams, S. J. Coles, P. N. Horton and S. J. A. Pope, *Inorg. Chem.*, 2014, **53**, 3788–3797; (e) M. Hee Lee, H. Mi Jeon, J. H. Han, N. Park, C. Kang, J. L. Sessler and J. Seung Kim, *J. Am. Chem. Soc.*, 2014, **136**, 8430–8437; (f) S. U. Hettiarachchi, B. Prasai and R. L. McCarley, *J. Am. Chem. Soc.*, 2014, **136**, 7575–7578; (g) X. Wu, X. Sun, Z. Guo, J. Tang, Y. Shen, T. D. James, H. Tian and W. Zhu, *J. Am. Chem. Soc.*, 2014, **136**, 3579–3588; (h) L. Zhang,

- D. Duan, Y. Liu, C. Ge, X. Cui, J. Sun and J. Fang, *J. Am. Chem. Soc.*, 2014, **136**, 226–233.
- 37 S. Banerjee, J. A. Kitchen, S. A. Bright, J. E. O'Brien, D. C. Williams, J. M. Kelly and T. Gunnlaugsson, *Chem. Commun.*, 2013, **49**, 8522–8524.
- 38 G. J. Ryan, R. B. P. Elmes, S. J. Quinn and T. Gunnlaugsson, *Supramol. Chem.*, 2012, **24**, 175–188.
- 39 (a) S. F. Yen, E. J. Gabbay and W. D. Wilson, *Biochemistry*, 1982, **21**, 2070–2076; (b) M. F. Braña, M. Cacho, M. A. Garcia, B. de Pascual-Teresa, A. Ramos, N. Acero, F. Llinares, D. Munoz-Mingarro, C. Abradelo, M. F. Rey-Stolle and M. Yuste, *J. Med. Chem.*, 2002, **45**, 5813–5816; (c) Q. Yang, P. Yang, X. Qian and L. Tong, *Bioorg. Med. Chem. Lett.*, 2008, **18**, 6210–6213; (d) K. J. Kilpin, C. M. Clavel, F. Edefe and P. J. Dyson, *Organometallics*, 2012, **31**, 7031–7039; (e) E. E. Langdon-Jones, N. O. Symonds, S. E. Yates, A. J. Hayes, D. Lloyd, R. Williams, S. J. Coles, P. N. Horton and S. J. A. Pope, *Inorg. Chem.*, 2014, **53**, 3788–3797; (f) J. M. Herrera, F. Mendes, S. Gama, I. Santos, C. Navarro Ranninger, S. Cabrera and A. G. Quiroga, *Inorg. Chem.*, 2014, **53**, 12627.
- 40 J. E. Rogers, S. J. Weiss and L. A. Kelly, *J. Am. Chem. Soc.*, 2000, **122**, 427–436.
- 41 K. A. Stevenson, S. F. Yen, N. C. Yang, D. W. Boykin and W. D. Wilson, *J. Med. Chem.*, 1984, **27**, 1677–1682.
- 42 H. K. Hariprakash, T. Kosakowska-Cholody, C. Meyer, W. M. Cholody, S. F. Stinson, N. I. Tarasova and C. J. Michejda, *J. Med. Chem.*, 2007, **50**, 5557–5560.
- 43 W. M. Cholody, T. Kosakowska-Cholody, M. G. Hollingshead, H. K. Hariprakash and C. J. Michejda, *J. Med. Chem.*, 2005, **48**, 4474–4481.
- 44 M. F. Brana and A. Ramos, *Curr. Med. Chem. Anti-Cancer Agents*, 2001, **1**, 237–255.
- 45 D. S. Tyson, C. R. Luman, X. Zhou and F. N. Castellano, *Inorg. Chem.*, 2001, **40**, 4063–4071.
- 46 G. F. Strouse, P. A. Anderson, J. R. Schoonover, T. J. Meyer and F. R. Keene, *Inorg. Chem.*, 1992, **31**, 3004–3006.
- 47 D. L. Reger, J. D. Elgin, R. F. Semeniuc, P. J. Pellechia and M. D. Smith, *Chem. Commun.*, 2005, 4068–4070.
- 48 D. L. Reger, J. Derek Elgin, P. J. Pellechia, M. D. Smith and B. K. Simpson, *Polyhedron*, 2009, **28**, 1469–1474.
- 49 J. Mehrotra, K. Misra and R. K. Mishra, *Indian J. Chem., Sect. B: Org. Chem. Incl. Med. Chem.*, 1993, **32**, 540–545.
- 50 P. A. Mabrouk and M. S. Wrighton, *Inorg. Chem.*, 1986, **25**, 526–531.
- 51 L. A. Kelly and M. A. J. Rodgers, *J. Phys. Chem.*, 1995, **99**, 13132–13140.
- 52 M. T. Carter, M. Rodriguez and A. J. Bard, *J. Am. Chem. Soc.*, 1989, **111**, 8901–8911.
- 53 B. Nordén, A. Rodger and T. Dafforn, *Linear Dichroism and Circular Dichroism: A Textbook on Polarized-light Spectroscopy*, Royal Society of Chemistry, 2010.
- 54 S. M. Cloonan, R. B. P. Elmes, M.-L. Erby, S. A. Bright, F. E. Poynton, D. E. Nolan, S. J. Quinn, T. Gunnlaugsson and D. C. Williams, *J. Med. Chem.*, 2015, **58**, 4494–4505.